Am. J. Hum. Genet. 74:1286–1293, 2004

Report

Disruption of *Contactin 4* (*CNTN4*) Results in Developmental Delay and Other Features of 3p Deletion Syndrome

Thomas Fernandez,[1,*] Thomas Morgan,[2,*] Nicole Davis,[1] Ami Klin,[1] Ashley Morris,[1] Anita Farhi,[2,3,4] Richard P. Lifton,[2,3,4] and Matthew W. State[1,2,3]

[1]Child Study Center, [2]Department of Genetics, [3]Yale Center for Human Genetics and Genomics, and [4]Howard Hughes Medical Institute, Yale University School of Medicine, New Haven

3p deletion syndrome is a rare contiguous-gene disorder involving the loss of the telomeric portion of the short arm of chromosome 3 and characterized by developmental delay, growth retardation, and dysmorphic features. All reported cases have involved, at a minimum, the deletion of chromosome 3 telomeric to the band 3p25.3. Despite the presence of several genes in this region that are involved in neural development, a causative relationship between a particular transcript and the observed clinical manifestations has remained elusive. We have identified a child with characteristic physical features of 3p deletion syndrome and both verbal and nonverbal developmental delay who carries a de novo balanced translocation involving chromosomes 3 and 10. Fine mapping of this rearrangement demonstrates that the translocation breakpoint on chromosome 3 falls within the recently identified minimal candidate region for 3p deletion syndrome and disrupts the *Contactin 4* (*CNTN4*) mRNA transcript at 3p26.2–3p26.3. This transcript (also known as *BIG-2*) is a member of the immunoglobulin super family of neuronal cell adhesion molecules involved in axon growth, guidance, and fasciculation in the central nervous system (CNS). Our results demonstrate the association of *CNTN4* disruption with the 3p deletion syndrome phenotype and strongly suggest a causal relationship. These findings point to an important role for *CNTN4* in normal and abnormal CNS development.

3p deletion syndrome is a rare contiguous-gene disorder involving the telomeric portion of the short arm of chromosome 3. Clinically, the syndrome is characterized by developmental delay, growth retardation, and dysmorphic features (Verjaal and De Nef 1978; Schwyzer et al. 1987; Narahara et al. 1990; Mowrey et al. 1993; Phipps et al. 1994; Drumheller et al. 1996; McClure et al. 1996; Angeloni et al. 1999; Benini et al. 1999; Cargile et al. 2002). Less commonly, renal cysts, gastrointestinal abnormalities, and congenital heart defects have been described. All reported cases involve, at a minimum, the loss of chromosomal material telomeric to 3p25.3. Terminal deletions involving the more centromeric regions of 3p have been thought to predispose to cardiac septal defects (Brand et al. 1987; Phipps et al. 1994; Drumheller et al. 1996; Green et al. 2000). However, a minimal candidate region conferring the common features of the syndrome has been identified recently in a patient with an interstitial deletion involving a 4.5-Mb interval between markers D3S3630 and D3S1304 (Cargile et al. 2002). Despite investigations of several genes in the 3p region involved in CNS development (Angeloni et al. 1999; Endris et al. 2002; Montag-Sallaz et al. 2003; Soderling et al. 2003), a causative relationship between any particular transcript and the range of observed clinical manifestations has remained elusive.

CT is a boy aged 7 years 11 mo with borderline intellectual functioning, distinctive facial (fig. 1) and other physical features, and behavioral problems who was seen in the Genetics Outpatient Clinic at Yale and evaluated under a research protocol approved by the Yale Human Investigation Committee with informed consent. The patient was the product of a nonconsanguineous union, delivered at 40 wk gestation from his 29 year-old primiparous mother by cesarean section performed because of failure to progress. There was no history of

Received December 29, 2003; accepted for publication March 29, 2004; electronically published April 21, 2004.

Address for correspondence and reprints: Dr. Matthew State, Yale Child Study Center and Department of Genetics, 230 South Frontage Road, New Haven, CT 06520. E-mail: Matthew.State@Yale.edu

* The first two authors contributed equally to this article.

0002-9297/2004/7406-0024$15.00

Figure 1 Eight-year-old boy with developmental delay and features of 3p deletion syndrome. The child has had surgical correction of prominent ptosis.

alcohol consumption or medication use during pregnancy and no known exposure to teratogens. He had a difficult facial presentation, with mild perinatal respiratory depression and an Apgar score of 3 at 1 min. Cord blood pH was 7.28. After brief positive pressure ventilation, his Apgar score was 9 at 5 min. Birth weight was 3,787 g and length was 19 inches. Cytogenetic analysis was performed shortly after birth, which revealed a balanced translocation (46, XY, t[3;10][p26;q26]) (fig. 2*A*). Both parents had normal karyotypes. No other family members were reported to have mental retardation or dysmorphic features.

The child's early motor development was unremarkable: he rolled over at 4 mo and was sitting with support at 6.5 mo. At 7 mo, he was able to stand with assistance, and he walked at 14 mo. His development of language, in contrast, was markedly delayed, with the absence of distinct single words until 3.5 years. CT underwent a cognitive assessment at age 7 years 2 mo and was found to have a full scale IQ of 73 on the Wechsler Intelligence Scale for Children, Third Edition (WISC-III) (Wechsler 1992) (Mean = 100; SD = 15), which places his cognitive skills within the borderline range of intellectual functioning. He obtained a verbal IQ of 81 and a performance (or nonverbal) IQ of 70. Significant weaknesses in his profile related to attention to visual detail (subtest score of 3; mean = 10, SD = 3), visual-spatial reconstruction skills (subtest score of 3), and understanding of social mores and expectations (subtest score of 3). These deficits contrasted with his significant strength in the area of fund of knowledge (subtest score of 12). An assessment of adaptive functioning at age 7 years 11 mo using the Vineland Adaptive Behavior Scales, Expanded Edition (Sparrow et al. 1984), showed marked impairments in social functioning and daily living skills. In the Daily Living Skills Domain, his percentile rank score was <0.1, corresponding to an age equivalent score of 4 years. In the Socialization Domain, his percentile rank score was within the first percentile, corresponding to an age equivalent score of 4 years 1 mo. Taken together, these findings demonstrated developmental delay, with particular deficits in nonverbal learning.

CT's past medical history was unremarkable. He was noted to be in excellent physical health and had required surgery only for correction of ptosis. He had been followed closely from a very young age by his pediatrician as a consequence of his dysmorphic features and known cytogenetic rearrangement and was not found to have any evidence of GI, cardiac, or renal abnormalities on physical exam or by history. A referral to a pediatric neurologist for behavioral issues at age 6 years revealed a normal neurological exam, except for the identification of mild hypotonia. Neither neuroimaging nor electroencephalogram was deemed to be clinically indicated.

Physical examination at age 7 years 11 mo revealed a height of 115.6 cm (5th–10th percentile), a weight of 21.4 kg (5th percentile), and a head circumference of 52 cm (50th–75th percentile). The patient showed high myopia and astigmatism, a low frontal hairline with right upsweep, forehead hypertrichosis, and bushy eyebrows without frank synophrys. He was also noted to have surgically improved ptosis and slight epicanthal folds, a broad nasal bridge with mild hypertelorism (measured at +1.5 SD at age 21 mo), downslanting palpebral fissures, downturned corners of the mouth, prominent but normal-sized ears with superior helices sagging downward, slight fifth-finger clinodactyly, branched transverse palmar crease of right hand, mild bilateral syndactyly of the second and third toes, hypertrichosis of his thighs and legs, and mild hypotonia. Deep tendon reflexes were normal.

The patient's clinical presentation, including developmental delay, growth retardation, and ptosis in combination with the known cytogenetic abnormality, sug-

gested a diagnosis of 3p deletion syndrome (table 1). Those physical signs not present in this case, such as trigonocephaly, microcephaly, and micrognathia, are not ubiquitous findings in other reported cases in the literature. The patient's particular cognitive findings are mirrored in at least one other case, described by Angeloni et al. (1999), in which the patient was found to have a full scale IQ in the borderline range with what appeared to be significant weaknesses in adaptive functioning. In addition, a marked delay in early language acquisition, as is seen in the present case, frequently has been noted anecdotally. However, a more detailed comparison of CT's cognitive findings with other reported cases is not possible, as a result of the informal descriptions of developmental delay that characterize the 3p deletion syndrome literature. What is apparent is that phenotypic variability in all aspects of the syndrome appears to be the rule rather than the exception. Moreover, genotype/phenotype relationships are not straightforward. For instance, as noted, there is a strong relationship between terminal deletions involving more proximal regions of chromosome 3 and cardiac findings (Brand et al. 1987; Phipps et al. 1994; Drumheller et al. 1996; Green et al. 2000). In contrast, the range and severity of dysmorphology and developmental delay may differ markedly in patients with similar, or even identical, deletions of

Table 1

Selected Features of 3p Deletion Syndrome

Features of 3p Deletion Syndrome	Affected Frequency[a] (%)	Status in the Presented Case[b]
Developmental delay	86	+
Postnatal growth retardation	86	+
Ptosis	77	+
Low birth weight	73	−
Malformed ears	68	+
Long philtrum	68	−
Broad nasal bridge	64	+
Hypotonia	50	+
Microcephaly	50	−
Micrognathia	50	−
Epicanthal folds	41	+
Post axial polydactyly	40	−
Hyperteliorism	36	+
Feeding problems	29	+
Clinodactyly	27	+
Trigonocephaly	23	−
Downturned corners of mouth	24	+
Synophoris	18	−
Low frontal hairline	14	+

[a] Frequency data is derived from the most recent and largest case review in the literature (Benini et al. 1999), consisting of 22 patients.

[b] + = present; − = absent.

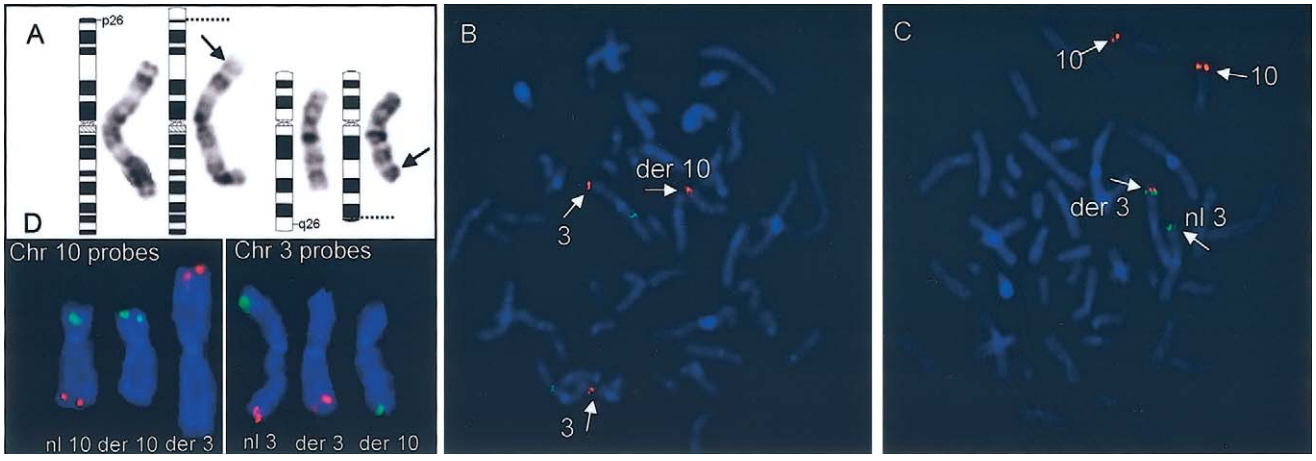

Figure 2 Cytogenetic and molecular cytogenetic studies of a de novo t(3;10) translocation. *A,* G-banded karyotype of the patient's lymphocytes showing a t(3p26;10q26) translocation. Arrows highlight the breakpoints on the respective chromosomes, and dotted lines show the corresponding position on the idiograms. 10/10 metaphase spreads examined showed the identical translocation. *B,* BAC probe 299N3 (*red*) spanning the chromosome 3p breakpoint. Hybridization signals are seen on both normal and derivative chromosomes 3. A third red hybridization signal is also seen on the derivative chromosome 10, as a result of the breakpoint transecting the region corresponding to the experimental probe. A control probe (*green*) maps to the q arm of chromosome 3. *C,* Probe 355F22 (*red*) spanning the chromosome 10q breakpoint. Hybridization signals are present on the normal and derivative chromosomes 10. A third red signal is seen on the telomeric region of chromosome 3. Control probes (*green*) map to the short arm of chromosome 3. *D,* Subtelomeric FISH results are shown. Chromosome 10 probes are in the left box—the normal (nl) chromosome 10 with both green and red probes, the derivative (der) 10 with only a green probe, and the derivative chromosome 3 with only the red probe are shown. The box on the right shows chromosome 3 probes, with the normal chromosome showing both red and green probes, the derivative 3 showing only the red probe, and the derivative 10 showing only the green probe.

the regions telomeric to 3p25.3 (Tazelaar et al. 1991; Knight et al. 1995; Benini et al. 1999).

Molecular studies were undertaken to fine map the (3;10) translocation using FISH, as described elsewhere (Lichter et al. 1990). Bacterial artificial chromosomes (BACs) corresponding to the observed cytogenetic bands involved in the apparently balanced translocation were identified using the UCSC genome browser and obtained from an RPCI-11 (Roswell Park Cancer Institute) library. These probes were hybridized to metaphase spreads consisting of the patient's lymphocytes. Several probes mapping centromeric and telomeric to the translocation breakpoints on both chromosomes were identified (table 2). Subsequent to the identification of BACs mapping on both sides of the translocation breakpoint on each chromosome, BACs within the translocation intervals were used, eventually identifying probes spanning both the chromosome 3 and 10 breakpoints (figs. 2 and 3). Two BACs spanning the chromosome 3 breakpoint, RPCI-11 299N33 and RPCI-11 121K9, were found to map in their entirety in the first intron of the gene *Contactin 4* (*CNTN4* [MIM 607280]) (fig. 3), establishing that the translocation breakpoint disrupted the gene within the 5′ UTR of the mature *CNTN4* mRNA. Importantly, *CNTN4* maps both within the minimal candidate region for 3p deletion syndrome defined by Cargile et al. (2002) and within a 6.7-cM region found linked to nonspecific mental retardation in large

Table 2

BAC Probes Investigated Using FISH

BAC ID	Base Position[a]	Chromosomal Band	Location Relative to Breakpoint
RP11-1082A18	chr3:10,298,689-10,516,466	3p25.3	Centromeric
RP11-572M14	chr3:10,011,785-10,180,797	3p25.3	Centromeric
RP11-1020A11	chr3:9,778,862-9,995,772	3p25.3	Centromeric
RP11-19E8	chr3:8,917,083-9,067,340	3p25.3	Centromeric
RP11-128A5	chr3:8,686,926-8,857,271	3p25.3	Centromeric
RP11-34L16	chr3:8,442,935-8,594,857	3p25.3	Centromeric
RP11-470E10	chr3:7,841,368-8,025,425	3p26.1	Centromeric
RP11-507D6	chr3:6,997,984-7,199,514	3p26.1	Centromeric
RP11-318I14	chr3:6,283,022-6,437,405	3p26.1	Centromeric
RP11-161L3	chr3:5,744,835-5,909,633	3p26.1	Centromeric
RP11-129J10	chr3:5,027,803-5,180,950	3p26.1	Centromeric
RP11-453A3	chr3:4,158,926-4,329,972	3p26.1	Centromeric
RP11-245A6	chr3:3,545,257-3,707,298	3p26.2	Centromeric
RP11-198P17	chr3:2,928,181-3,117,274	3p26.2	Centromeric
RP11-94M9	chr3:2,804,247-2,975,122	3p26.2	Centromeric
RP11-785A7	chr3:2,690,183-2,862,993	3p26.2–3p26.3	Centromeric
RP11-82O3	chr3:2,566,282-2,742,197	3p26.3	Centromeric
RP11-63O1	chr3:2,443,361-2,617,387	3p26.3	Centromeric
RP11-211K13	chr3:2,307,996-2,470,413	3p26.3	Centromeric
RP11-762O12	chr3:2,287,581-2,441,071	3p26.3	Centromeric
RP11-299N3	chr3:2,181,279-2,367,269	3p26.3	Spanning
RP11-129K1	chr3:2,132,133-2,290,752	3p26.3	Spanning
RP11-176P14	chr3:2,021,987-2,193,951	3p26.3	Telomeric
RP11-416N8	chr3:1,244,095-1,420,317	3p26.3	Telomeric
RP11-392M7	chr3:1,064,436-1,252,749	3p26.3	Telomeric
RP11-114K9	chr3:333,643-518,322	3p26.3	Telomeric
RP11-306H5	chr3:159,323-343,406	3p26.3	Telomeric
RP11-338L11	chr10:116,448,883-116,645,816	10q25.3	Centromeric
RP11-169K19	chr10:117,157,040-117,301,164	10q25.3	Centromeric
RP11-96N16	chr10:117,471,461-117,637,580	10q25.3	Centromeric
RP11-295023	chr10:117,733,868-117,949,898	10q25.3	Centromeric
RP11-498B4	chr10:118,011,104-118,209,364	10q25.3	Centromeric
RP11-5G18	chr10:118,364,598-118,528,414	10q25.3–10q26.11	Centromeric
RP11-328K15	chr10:119,130,080-119,172,006	10q26.11	Centromeric
RP11-355F22	chr10:119,170,007-119,301,205	10q26.11	Spanning
RP11-136I7	chr10:119,181,243-119,340,828	10q26.11	Spanning
RP11-280F22	chr10:119,299,202-119,400,731	10q26.11	Telomeric
RP11-3H12	chr10:119,316,263-119,394,906	10q26.11	Telomeric
RP11-354M20	chr10:119,398,732-119,592,400	10q26.11	Telomeric

[a] Derived from the July 2003 freeze of the Human Genome Project.

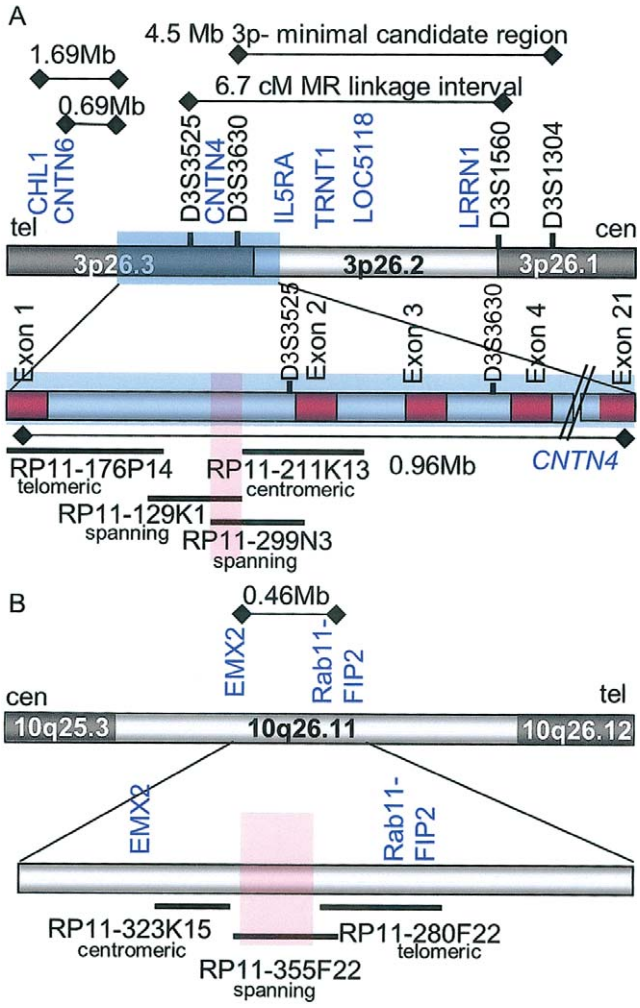

Figure 3 Diagram of chromosomes 3 and 10 breakpoints. *A*, Telomeric region of chromosome 3 from 3p26.1 to 3p26.3, represented by the grey and white bar at the top of the diagram. Relevant STS markers are in black text, and known genes from the RefSeq database are in blue text. The region corresponding to *CNTN4* is pictured as a blue shaded rectangle. Distances noted were derived from the July 2003 freeze of the Human Genome Project and include: (1) the 1.69 Mb-interval from the 3′-most exon of CHL1 to exon 1 of CNTN4; (2) the 0.69-Mb interval from the 3′-most exon of CNTN6 to exon 1 of CNTN4; (3) the 4.5-Mb interval defined by Cargile et al. (2002) as the smallest interstitial deletion identified in a 3p deletion syndrome case; and (4) the 6.7-cM interval identified by Higgins et al. (2002) in a large pedigree affected with nonspecific mental retardation (Z_{max} = 9.18 at marker D3S3050). The bar below the genomic interval shows detail of the region, including exons of *CNTN4* (*in red*). Selected BACs are noted as dark horizontal bars beneath. The breakpoint interval is shown as a red rectangle. The position of each BAC probe relative to the breakpoint on chromosome 3 is indicated below the RPCI-11 library identifier. The distance for the entire genomic interval corresponding to *CNTN4* is indicated below the thin black line. *B*, Chromosome 10 in the region from 10q25.3-10q26.12, represented by the grey and white bar at the top of the diagram. Known genes from the RefSeq database are noted in blue. The 0.46-Mb distance between the 3′-most exon of EMX2 and the 5′-most exon of Rab11-FIP2 was determined by the July 2003 freeze of the Human Genome Project. The lower bar shows details of the interval, with the relative position of known genes in the region in blue text. The breakpoint region is highlighted with a red rectangle. No known genes or spliced ESTs were identified on the BAC spanning the chromosome 10 breakpoint. BACs from the region are identified as dark horizontal lines below the genomic region, with their position relative to the breakpoint on chromosome 10 noted below their RPCI identifiers.

kindred (Z_{max} = 9.18 at marker D3S3050) (Higgins et al. 2000) (fig. 3*A*).

BACs RPCI-11 355F22 (figs. 2 and 3) and RPCI-11 136I7 were found to span the chromosome 10 translocation breakpoint. This chromosome segment lies within a gene-poor region in the band 10q26.11(fig. 3*B*). No known or predicted transcripts or spliced ESTs were identified on these clones with the use of the UCSC genome browser. Five distinct ESTs without canonical splice sites were mapped to the BAC. Efforts to extend these fragments *in silico* with the use of the BLAST server at the National Center for Biotechnology Information

were unsuccessful, and four of these five fragments showed no significant homology to other human ESTs or known genes. One region at the far telomeric extent of BAC 355F22 contained a block of 444 bp of DNA showing >95% homology at the nucleotide level to the tyrosine 3-monooxygenase/tryptophan 5-monooxygenase activation protein, theta polypeptide (*YWHAQ* [accession number BC050601]) on chromosome 2 as well as the *YWHAQ* pseudogene 2 on chromosome 22 (accession number NM_006826). No additional sequences with homology to *YWHAQ* were identified in the chromosome 10 interval via BLAST or BLAT searches. These analyses do not exclude the possibility of a rare transcript mapping to the 10q breakpoint region. However, the characteristic physical features in this case point to the chromosome 3 region as the proximate cause of the patient's presentation.

Additional FISH studies were undertaken to evaluate the regions telomeric and centromeric to the 3p translocation (table 2). These resulted in no evidence of a deletion. Subtelomeric FISH with the use of commercially available probes was also performed to confirm the integrity of the terminal regions of the normal and derivative chromosomes 3 and 10 (fig. 2*D*). FISH mapping of BACs corresponding to the two closest transcripts on the telomeric aspect of the breakpoint, *CHL1* (*Close Homologue of L1*, also known as *CALL* [MIM 607416]) and *CNTN6* (MIM 607220), each showed the expected pattern of two hybridization signals, and direct sequencing of *CNTN4* in the patient demonstrated no mutations in the coding regions of the remaining, intact transcript (data not shown).

The finding of disruption of *CNTN4* is of particular interest as this gene encodes a neuronal adhesion molecule that is a member of the immunoglobulin (Ig) superfamily of genes. Similar to other members of the contactin family, which includes F3/F11/contactin (MIM 600316), *TAG-1* (*CNTN2* [MIM 190197]), *BIG-1* (*CNTN3* [MIM 601325]), *NB-2* (*CNTN5* [MIM 607219]), and *NB-3* (*CNTN6*), full-length *CNTN4* consists of six immunoglobulin domains and four fibronectin III (FNIII) domains and is anchored to the cell membrane via a glycosylphosphatidyl-inositol (GPI) domain. This family of proteins have been shown to be involved in axon growth, guidance, and fasciculation (Yoshihara et al. 1995; Ogawa et al. 1996; Saito et al. 1998; Kamei et al. 2000) and have been proposed to have a role in synaptic plasticity (Murai et al. 2002). A specific role for *CNTN4* in neuronal development has not yet been clarified. However, knockouts of homologous neuronal adhesion molecules in mouse have resulted in viable mutants demonstrating morphological, neurological, and behavioral abnormalities (Berglund et al. 1999; Montag-Sallaz et al. 2002; Montag-Sallaz et al. 2003; Rolf et al. 2003).

At present, three isoforms of *CNTN4* are described in the RefSeq database at NCBI. The identified breakpoint in this case disrupts only the longest variant which is highly expressed in human brain, particularly in cerebellum, thalamus, amygdala, and cerebral cortex (Kamei et al. 2000; Zeng et al. 2002). An intermediate-sized isoform, consisting of three Ig domains and three FNIII domains, has not been found to be expressed in the CNS (Kamei et al. 2000; Zeng et al. 2002; Hansford et al. 2003). A third, markedly truncated variant lacking all six Ig domains and two of the four FNIII domains has been shown to have low levels of expression in the brain, on the basis of northern blot and RT-PCR analysis (Zeng et al. 2002).

Given the inaccessibility of the relevant tissue, we were not able to test directly whether the translocation altered expression of the short brain-expressed variant, despite that transcript remaining structurally intact. Several characteristics of the full-length isoform, however, point to the clearly disrupted variant as the key determinant in the present case, irrespective of the status of the alternative transcript. First, the long variant is the only known isoform that codes for six Ig-like domains and four FNIII domains, reflecting the canonical structure of CNTN proteins. Studies of the contactin gene family have revealed a complex pattern of homophilic and heterophilic interactions that are required for axon growth and pathfinding. Such studies demonstrate that these essential functions are mediated by the combination and juxtaposition of multiple Ig and FNIII domains. Second, these neuronal adhesion molecules demonstrate highly regulated temporal and spatial expression patterns in the CNS. For this reason, the disruption of the regulatory region of the predominant brain-expressed isoform reasonably would be expected to have significant functional consequences. Third, the smaller brain-expressed variant, *CNTN4a*, demonstrates low levels of expression that are confined to the cerebral cortex, thus minimally overlapping with that of the long isoform (Zeng et al. 2002). These factors in combination with the lack of all Ig and several FNIII domains suggest that this truncated gene product would be a poor candidate to compensate for disruption of the full-length isoform. Finally, the clinical overlap in this case with findings from cases of frank deletion of the terminal region of chromosome 3p supports the hypothesis that the interruption of the long variant alone is sufficient to result in functional haploinsufficiency at this locus.

The region telomeric to the disrupted *CNTN4* gene contains *CNTN6* and *CHL1*, both neuronal cell adhesion molecules that also contain Ig and FNIII domains (fig. 3). Of note, a patient with nonspecific mental retardation and a balanced translocation disrupting *CHL1* was described elsewhere (Frints et al. 2003). This patient was not found to have any other physical abnormalities

associated with 3p deletion syndrome, and the translocation also involved the X chromosome, though no transcript was identified at that breakpoint. Analyses of *CHL1* knockout mice, in this study and in others, have identified anomalies in axonal organization in various brain regions, as well as subtle behavioral abnormalities in homozygous null animals (Montag-Sallaz et al. 2002, 2003; Frints et al. 2003).

Given the proximity of these brain-expressed molecules with similar structures and putative functions, it is conceivable that the chromosomal rearrangement leading to disruption of *CNTN4* could also be mediating functional consequences for neighboring transcripts and, thereby, leading to the observed phenotype. Although the possibility of position effect cannot be excluded on the basis of current data (State et al. 2003), the direct disruption of the *CNTN4* transcript and the genomic distances separating *CNTN6* and *CHL1* from the breakpoint (~0.7 Mb and ~1.7Mb, respectively) suggest that the most likely effect of the rearrangement is on *CNTN4* function. Moreover, two additional lines of evidence support a specific role for *CNTN4* in conferring the observed phenotype. First, in the single reported case of a translocation disrupting *CHL1*, the patient did not show dysmorphic features consistent with 3p deletion syndrome (Frints et al. 2003), and, second, the 3p minimal candidate region (Cargile et al. 2002) includes the *CNTN4* transcript, but not *CNTN6* and *CHL1* (fig. 3*A*), suggesting that position effect would have to be invoked as an explanation in both the interstitial deletion and translocation cases.

Our findings strongly suggest that disruption of a single copy of *CNTN4* is sufficient to confer key aspects of the 3p deletion syndrome phenotype, including developmental delay. Thus, *CNTN4* is one of a relatively small number of autosomal genes identified as contributing to cognitive deficits in a contiguous-gene syndrome. It is interesting to note that many features of a presumed multigene phenotype are manifested as the result of the disruption of only a single transcript. This finding provides a rationale for mutation screening of *CNTN4* in selected patients with developmental delay and dysmorphic features who have normal karyotypes. Although, in the present case, there appears to be a strong relationship between alterations in *CNTN4* expression and characteristic physical findings, nonetheless, it is noteworthy that a previous analysis of an extended pedigree identified evidence for a recessive locus conferring nonspecific mental retardation within a 7-cM region containing *CNTN4* (Higgins et al. 2000). On the basis of the present findings, this gene should certainly be considered a candidate transcript in the linkage interval. Finally, it is particularly interesting that the patient's developmental difficulties involve notable weaknesses in nonverbal aspects of learning as well as a delay in language acquisition. The identification of a likely etiological role for *CNTN4* in these types of human cognitive deficits suggests that further studies of its expression and specific functions in the CNS are warranted.

Acknowledgments

The work was funded by a grant from the Shepherd Foundation (M.W.S.) as well as an National Institutes of Health career award (RR-16118 to M.W.S.). The authors wish to thank George and Lynn Bovenizer, whose support was instrumental in the conduct of this research. The authors would also like to thank Fred Volkmar for his continuing collaboration and Celine Saulnier, Eunice Huang, and Reid Warner of the Developmental Disabilities Clinic at the Yale Child Study Center for their highly skilled clinical assistance. Finally, we express our deepest gratitude to the patient and his family for their participation in this research.

Electronic-Database Information

Accession numbers and URLs for data presented herein are as follows:

Basic Local Alignment Search Tool (BLAST), http://www.ncbi.nlm.nih.gov/BLAST/
BLAT Search Genome, http://genome.ucsc.edu/cgi−bin/hgBlat
National Center for Biotechnology Information (NCBI), http://www.ncbi.nlm.nih.gov/
NCBI Reference Sequence (RefSeq), http://www.ncbi.nlm.nih.gov/RefSeq
Online Mendelian Inheritance in Man (OMIM), http://www.ncbi.nlm.nih.gov/Omim
UCSC Genome Browser, http://genome.ucsc.edu

References

Angeloni D, Lindor NM, Pack S, Latif F, Wei MH, Lerman MI (1999) CALL gene is haploinsufficient in a 3p− syndrome patient. Am J Med Genet 86:482–485

Benini D, Vino L, Vecchini S, Fanos V (1999) 46, XY, del (3) (pter→p25) syndrome: further delineation of the clinical phenotype. Eur J Pediatr 158:955–957

Berglund EO, Murai KK, Fredette B, Sekerkova G, Marturano B, Weber L, Mugnaini E, Ranscht B (1999) Ataxia and abnormal cerebellar microorganization in mice with ablated contactin gene expression. Neuron 24:739–750

Brand A, Reifen RM, Armon Y, Kerem E, Horenstein E, Gale R (1987) Double mitral valve, complete atrioventricular canal, and tricuspid atresia in chromosomal 3p− syndrome. Pediatr Cardiol 8:55–56

Cargile CB, Goh DL, Goodman BK, Chen XN, Korenberg JR, Semenza GL, Thomas GH (2002) Molecular cytogenetic characterization of a subtle interstitial del(3)(p25.3p26.2) in a patient with deletion 3p syndrome. Am J Med Genet 109: 133–138

Drumheller T, McGillivray BC, Behrner D, MacLeod P, McFadden DE, Roberson J, Venditti C, Chorney K, Chorney

M, Smith DI (1996) Precise localisation of 3p25 breakpoints in four patients with the 3p− syndrome. J Med Genet 33: 842–847

Endris V, Wogatzky B, Leimer U, Bartsch D, Zatyka M, Latif F, Maher ER, Tariverdian G, Kirsch S, Karch D, Rappold GA (2002) The novel Rho-GTPase activating gene MEGAP/srGAP3 has a putative role in severe mental retardation. Proc Natl Acad Sci USA 99:11754–11759

Frints SG, Marynen P, Hartmann D, Fryns JP, Steyaert J, Schachner M, Rolf B, Craessaerts K, Snellinx A, Hollanders K, D'Hooge R, De Deyn PP, Froyen G (2003) CALL interrupted in a patient with non-specific mental retardation: gene dosage-dependent alteration of murine brain development and behavior. Hum Mol Genet 12:1463–1474

Green EK, Priestley MD, Waters J, Maliszewska C, Latif F, Maher ER (2000) Detailed mapping of a congenital heart disease gene in chromosome 3p25. J Med Genet 37:581–587

Hansford LM, Smith SA, Haber M, Norris MD, Cheung B, Marshall GM (2003) Cloning and characterization of the human neural cell adhesion molecule, CNTN4 (alias BIG-2). Cytogenet Genome Res 101:17–23

Higgins JJ, Rosen DR, Loveless JM, Clyman JC, Grau MJ (2000) A gene for nonsyndromic mental retardation maps to chromosome 3p25-pter. Neurology 55:335–340

Kamei Y, Takeda Y, Teramoto K, Tsutsumi O, Taketani Y, Watanabe K (2000) Human NB-2 of the contactin subgroup molecules: chromosomal localization of the gene (CNTN5) and distinct expression pattern from other subgroup members. Genomics 69:113–119

Knight LA, Yong MH, Tan M, Ng IS (1995) Del(3) (p25.3) without phenotypic effect. J Med Genet 32:994–995

Lichter P, Tang CJ, Call K, Hermanson G, Evans GA, Housman D, Ward DC (1990) High-resolution mapping of human chromosome 11 by in situ hybridization with cosmid clones. Science 247:64–69

McClure RJ, Telford N, Newell SJ (1996) A mild phenotype associated with der(9)t(3;9) (p25;p23). J Med Genet 33: 625–627

Montag-Sallaz M, Baarke A, Montag D (2003) Aberrant neuronal connectivity in CHL1-deficient mice is associated with altered information processing-related immediate early gene expression. J Neurobiol 57:67–80

Montag-Sallaz M, Schachner M, Montag D (2002) Misguided axonal projections, neural cell adhesion molecule 180 mRNA upregulation, and altered behavior in mice deficient for the close homolog of L1. Mol Cell Biol 22:7967–7981

Mowrey PN, Chorney MJ, Venditti CP, Latif F, Modi WS, Lerman MI, Zbar B, Robins DB, Rogan PK, Ladda RL (1993) Clinical and molecular analyses of deletion 3p25-pter syndrome. Am J Med Genet 46:623–629

Murai KK, Misner D, Ranscht B (2002) Contactin supports synaptic plasticity associated with hippocampal long-term depression but not potentiation. Curr Biol 12:181–190

Narahara K, Kikkawa K, Murakami M, Hiramoto K, Namba H, Tsuji K, Yokoyama Y, Kimoto H (1990) Loss of the 3p25.3 band is critical in the manifestation of del(3p) syndrome: karyotype-phenotype correlation in cases with deficiency of the distal portion of the short arm of chromosome 3. Am J Med Genet 35:269–273

Ogawa J, Kaneko H, Masuda T, Nagata S, Hosoya H, Watanabe K (1996) Novel neural adhesion molecules in the Contactin/F3 subgroup of the immunoglobulin superfamily: isolation and characterization of cDNAs from rat brain. Neurosci Lett 218:173–176

Phipps ME, Latif F, Prowse A, Payne SJ, Dietz-Band J, Leversha M, Affara NA, Moore AT, Tolmie J, Schinzel A, Lerman MI, Ferguson-Smith MA, Maher ER (1994) Molecular genetic analysis of the 3p− syndrome. Hum Mol Genet 3: 903–908

Rolf B, Lang D, Hillenbrand R, Richter M, Schachner M, Bartsch U (2003) Altered expression of CHL1 by glial cells in response to optic nerve injury and intravitreal application of fibroblast growth factor-2. J Neurosci Res 71:835–843

Saito H, Mimmack M, Kishimoto J, Keverne EB, Emson PC (1998) Expression of olfactory receptors, G-proteins and AxCAMs during the development and maturation of olfactory sensory neurons in the mouse. Brain Res Dev Brain Res 110:69–81

Schwyzer U, Binkert F, Caflisch U, Baumgartner B, Schinzel A (1987) Terminal deletion of the short arm of chromosome 3, del(3pter-p25): a recognizable syndrome. Helv Paediatr Acta 42:309–315

Soderling SH, Langeberg LK, Soderling JA, Davee SM, Simerly R, Raber J, Scott JD (2003) Loss of WAVE-1 causes sensorimotor retardation and reduced learning and memory in mice. Proc Natl Acad Sci USA 100:1723–1728

Sparrow S, Balla D, Cicchetti D (1984) Vineland adaptive behavior scales, expanded ed. American Guidance Service, Circle Pines, MN

State MW, Greally JM, Cuker A, Bowers PN, Henegariu O, Morgan TM, Gunel M, DiLuna M, King RA, Nelson C, Donovan A, Anderson GM, Leckman JF, Hawkins T, Pauls DL, Lifton RP, Ward DC (2003) Epigenetic abnormalities associated with a chromosome 18(q21-q22) inversion and a Gilles de la Tourette syndrome phenotype. Proc Natl Acad Sci USA 100:4684–4689

Tazelaar J, Roberson J, Van Dyke DL, Babu VR, Weiss L (1991) Mother and son with deletion of 3p25-pter. Am J Med Genet 39:130–132

Verjaal M, De Nef MB (1978) A patient with a partial deletion of the short arm of chromosome 3. Am J Dis Child 132: 43–45

Wechsler D (1992) Wechsler intelligence scale for children, 3rd ed (WISC-III). Psychological Corporation, San Antonio, TX

Yoshihara Y, Kawasaki M, Tamada A, Nagata S, Kagamiyama H, Mori K (1995) Overlapping and differential expression of BIG-2, BIG-1, TAG-1, and F3: four members of an axon-associated cell adhesion molecule subgroup of the immunoglobulin superfamily. J Neurobiol 28:51–69

Zeng L, Zhang C, Xu J, Ye X, Wu Q, Dai J, Ji C, Gu S, Xie Y, Mao Y (2002) A novel splice variant of the cell adhesion molecule contactin 4 (CNTN4) is mainly expressed in human brain. J Hum Genet 47:497–499